Proceedings of the 12th IEEE International
Conference on Nano/Micro Engineered and Molecular Systems
April 9-12, 2017, Los Angeles, USA

Pneumatic Microvalves Fabricated by Multi-material 3D Printing

Xue Jiang and Peter B. Lillehoj
Department of Mechanical Engineering
Michigan State University
East Lansing, USA

***Abstract*—We report an innovative and simple approach for fabricating pneumatic microvalves via an assembly-free 3D printing technique. These valves are based on monolithic elastomeric valves fabricated by multilayer soft lithography but this method circumvents the need for specialized layering, alignment and bonding. 3D printed microfluidic devices containing flow channels and pneumatic valves were fabricated and tested for functionality. Using these devices, we successfully demonstrate valve actuation for precise liquid flow control and on/off operation. The speed and simplicity of this approach make it a promising technique for rapid prototyping and manufacturing of 3D printed microfluidic devices with fully integrated components.**

Keywords—microfluidics; microvalves; 3D printing; multi-material

INTRODUCTION

Microfluidics has become a revolutionary technology in many important fields including molecular biology [1-3], analytical chemistry [4, 5] and drug discovery [6, 7]. To date, poly(dimethylsiloxane) (PDMS) has been exclusively used for prototyping microfluidic devices due to its rapid fabrication, low cost and favorable material properties [8]. One of the earliest and most popular methods for fabricating PDMS microdevices is soft lithography, which is based on a replica molding process [9-11]. As an extension of this technology, multilayer soft lithography enables the rapid fabrication of microfluidic components such as valves and pumps [12]. While capable of generating functional devices, multilayer soft lithography generally relies on microfabricated silicon molds and involves specialized layering, alignment and bonding steps. Therefore, new techniques to rapidly manufacture microfluidic devices that are less laborious are desired. Recently, 3D printing has emerged as a promising platform for prototyping microfluidic devices due to its speed and simplicity [13-16]. Several groups have reported the fabrication of microfluidic components, including valves, pumps and multiplexers, using stereolithography (SL) [17-20]. While useful, these approaches require a separate build substrate or precise control of the light curing process. Here, we demonstrate fully integrated microfluidic valves fabricated via fused deposition modeling (FDM) which is the most widely used 3D printing technology.

MATERIALS AND METHODS

Device Design

Microfluidic devices were designed using Siemens NX software and PRT files were exported to STL for 3D printing. Each device is comprised of three layers consisting of a 1.7 mm-thick elastomer layer sandwiched between two 500 μm-thick rigid plastic layers (Fig. 1a). A flow channel, with a width of 500 μm and height of 200 μm, is for a liquid sample (Fig. 1b) and control channels, having widths of 500 μm, 750 μm, 1000 μm and a height of 200 μm, are for compressed gas (Fig. 1c). The flow and control channels are configured in a cross-channel architecture, forming valves at their intersections. The thickness of the elastomer membrane at these intersections is 20 μm and the overall device dimensions are 2 mm × 2 mm.

Fabrication Process

Microfluidic devices were printed using an Objet Connex350 multi-material 3D printer (Stratasys Ltd., Eden Prairie, MN). The elastomer layer was printed using TANGOBLACKPLUS FLX980, a rubber-like material, and the rigid layers were printed using VEROCLEAR RGD810, a transparent thermoplastic. Relevant properties of these materials are presented in Table 1. SUPPORT SUP705 was used for the support material. During the printing process, the elastomer and plastic layers are simultaneously printed and fused together resulting in a strong, leak-free bond. A single device can be printed in ~35 min.

Table 1. Relevant properties of 3D printed materials

	Polymerized density (g/cm^3)	Shore Hardness	Tensile strength (MPa)
TANGOBLACKPLUS FLX980	1.12-1.13	26-28 (Scale A)	0.8-1.5
VEROCLEAR RGD810	1.18-1.19	83-86 (Scale D)	50-65

After the devices were printed, the support material was physically extracted using a 22 gauge needle. Devices were then soaked in a 2wt% NaOH solution for 2 hr to remove residual support material, followed by drying under a stream of purified N_2 gas. PVC tubing was connected to the inlets/outlets using pieces of 0.028 in-diameter stainless steel tubing, which were glued to the device using epoxy (J-B Weld, Sulphur

Springs, TX). PVC and stainless steel tubing were purchased from McMaster-Carr (Elmhurst, IL).

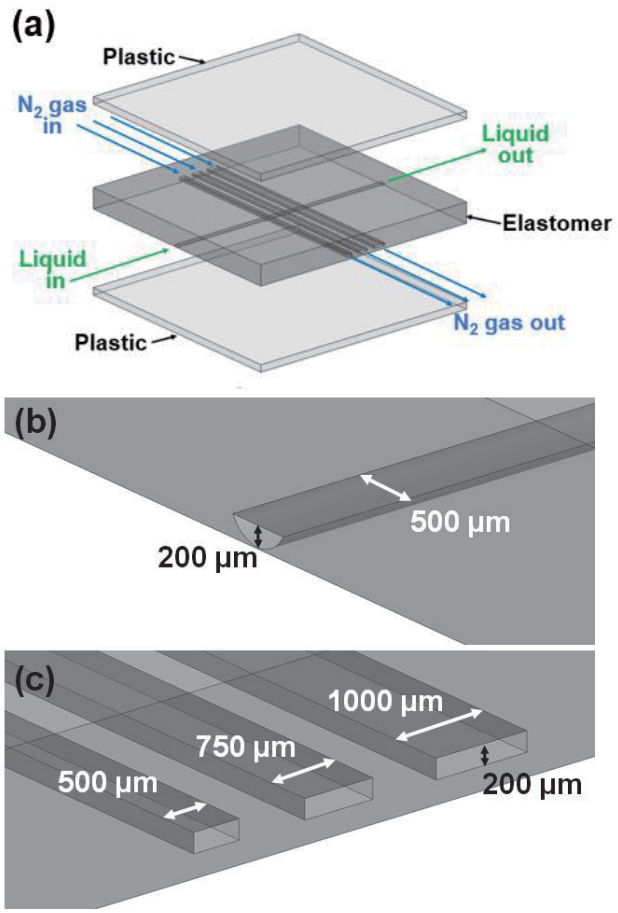

Figure 1. (a) Exploded view of the 3D printed microvalves. The flow and control channels are configured in a cross-channel architecture, forming valves at their intersections. Close-up views of the flow channel (b) and control channels (c).

Experimental Setup

A photograph of the 3D printed microfluidic device during testing is shown in Fig. 2. The inlets of the control channels were coupled together using plastic tees (McMaster-Carr) and connected to a compressed N_2 cylinder via a Fisherbrand pressure regulator. The control channel outlets were connected to PVC tubing which were open to the atmosphere or blocked with a stainless steel plug. The flow channel inlet was connected to a KD Scientific syringe pump (Holliston, MA) and the outlet was fed to a waste container via PVC tubing. To better visualize the liquid flow, colored dye, prepared by diluting food coloring with deionized (DI) water, was pumped inside the flow channel. Optical images were captured using a Nikon ECLIPSE TS100 inverted microscope (Melville, NY) and processed using NIS-Elements software.

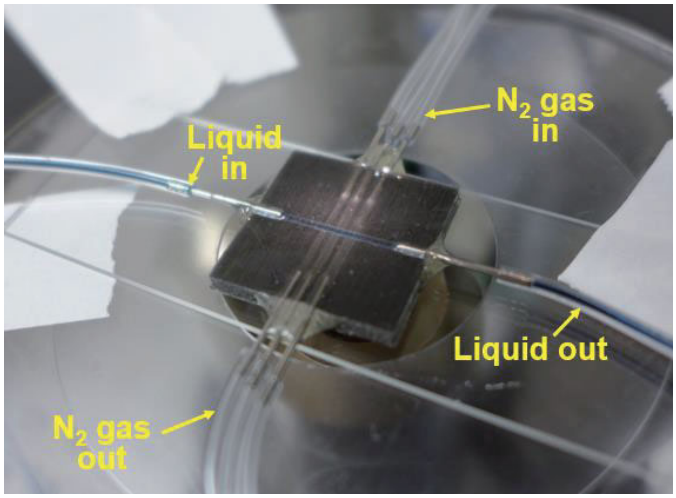

Figure 2. Photograph of the 3D printed microfluidic device. The flow channel is connected to a syringe pump with colored dye and the control channels are connected to compressed N_2 gas via a pressure regulator.

Valve Operation and Characterization

Valves were actuated by manually adjusting the N_2 pressure via the pressure regulator. For all measurements, we started with a gas pressure of 0 psi (gage) and increased it by 0.5 psi increments. The pressure at each interval was held for 5 sec before being increased to allow sufficient time for the system to stabilize. We first characterized the valves by measuring the fractional valve opening at different gas pressures with the flow channel open to the atmosphere. For these experiments, we used microfluidic devices with a single control channel having a width of 500 µm, 750 µm or 1000 µm. Devices were positioned vertically under the microscope to allow the light to shine through the flow channel. As the valve was actuated, the resulting cross sectional area was measured. We calculated the fractional valve opening by dividing the actuated cross sectional area of the flow channel by its cross sectional area when fully opened (at 0 psi). Each measurement was repeated twice using the same device.

For liquid flow rate measurements, we used devices with three control channels (Fig. 1) and plugged one of them, leaving the other two channels open to the atmosphere. Since the three control channels are independent, only the plugged channel is actuated. Colored dye was pumped through the flow channel at a flow rate of 0.05 mL/min. To determine the liquid flow rate at different actuation pressures, we first measured the distance travelled by the liquid in the plastic tubing at two time intervals. Using the dimensions of the tubing, we calculated the volume of liquid and divided it by time interval to obtain the volumetric flow rate. Each measurement was repeated twice using the same device.

Results and Discussion

To evaluate the functionality of our 3D printed valves, we first observed their actuation performance using colored dye. As shown in Fig. 3, the closing of the valves can be clearly

observed at the intersections between the flow (horizontal) and control (vertical) channels. The expansion of the control channel due to the compressed gas results in a uniform pressure on the flow channel, causing the liquid inside to be squeezed out. By using colored dye, the closing of the valves can be easily visualized by observing the color at the channel intersection. Since the gas pressure to close the valves is inversely proportional to the channel width, the largest valve is closed at the lowest pressure while the smaller valves remain partially open (Fig. 3b). As the gas pressure is increased, the smaller valves are sequentially closed (Figs. 3c, d). It is important to note that the valves are fully closed only when no dye is present inside the flow channel. Even a slight hint of coloring in the flow channel indicates liquid flow. For example, while the 500 µm-wide valve appears fully closed at 9 psi (Fig. 3c), there is still a small amount of coloring which indicates that there is liquid travelling through the channel. At 12 psi (Fig. 3d), the flow channel is colorless, which indicates that it is fully closed.

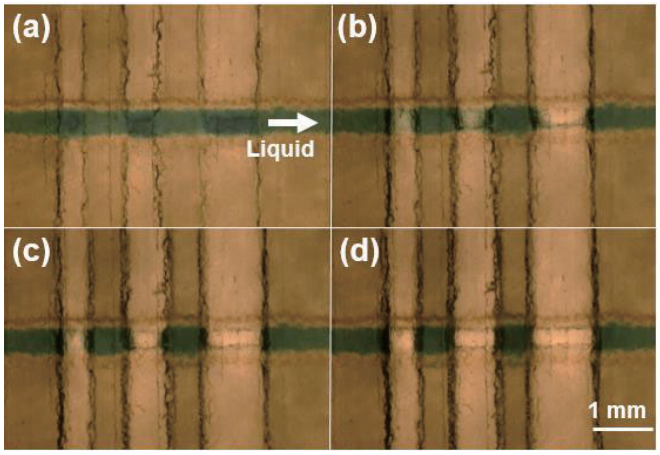

Figure 3. Optical images of valves with widths of 500 µm, 750 µm and 1000 µm (left to right) at 0 psi (a), 6 psi (b), 9 psi (c), and 12 psi (d). The flow channel is filled with colored dye for improved visualization.

To further evaluate the performance of these valves, we measured the fractional valve opening at various actuation pressures. As shown in Fig. 4, all three valve sizes exhibit a significant drop in the opening area at only 1 psi, which is likely due to the small thickness and high elasticity of the elastomer membrane. At higher pressures, the closing of the valves is proportional to the applied pressure and the 500 µm, 750 µm and 1000 µm-wide valves are fully closed at 8 psi, 5 psi, 4 psi, respectively. Since these experiments are performed when the flow channel is open to the atmosphere, the pressures required to fully close the valves are ~1/3 smaller than when the channel is filled with colored dye (Fig. 3).

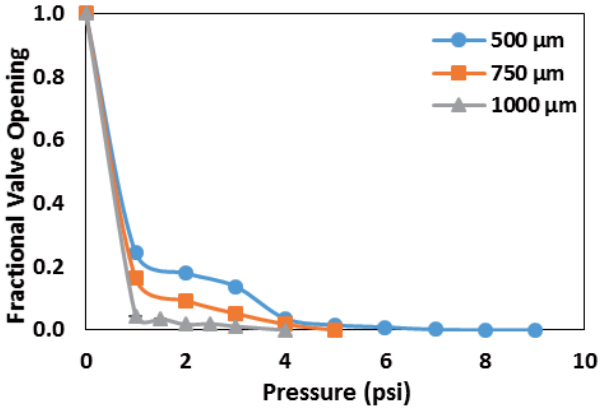

Figure 4. Fractional valve opening *vs*. gas pressure for valve widths of 500 µm, 750 µm and 1000 µm. Measurements were performed with the flow channel open to atmosphere. Each data point represents the mean ± standard deviation (SD) of two measurements.

We also performed experiments to evaluate the effectiveness of these values for fluidic control. For this study, colored dye was pumped through the flow channel and the liquid flow rate was measured at different valve actuation pressures. As shown in Fig. 5, the flow rate is proportional to the gas pressure for all three valve sizes. Additionally, the measured pressures at which the valves were fully closed are consistent with the pressures observed in the optical images (Fig. 3). The data exhibits very good reproducibility, however, there are a few data points with larger standard deviations which we attribute to experimental error in timing the distance travelled by the liquid in the tubing. Nonetheless, these results show that our 3D printed valves can be used to reliably control the flow rate as well as fully stop the flow.

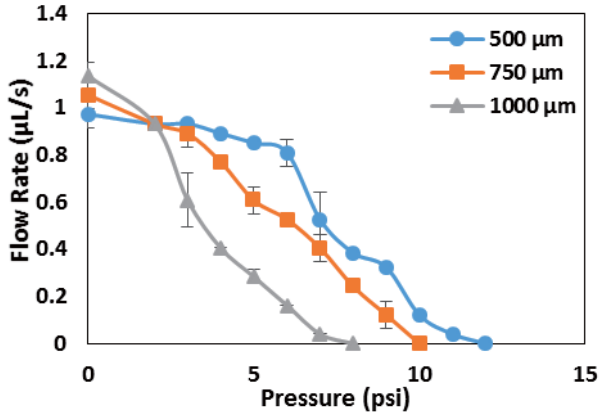

Figure 5. Liquid flow rate *vs*. gas pressures for valve widths of 500 µm, 750 µm and 1000 µm. Measurements were performed with colored dye pumped through the flow channel at a rate of 0.05 mL/min. Each data point represents the mean ± SD of two measurements.

CONCLUSIONS

We have demonstrated an assembly-free technique for fabricating microfluidic devices and components via multi-material 3D printing. This approach is based on fused deposition modeling (FDM) technology and allows multiple types of materials to be simultaneously printed. For proof-of-concept, we use this technique to fabricate multilayer pneumatic microvalves. Experiments were performed to characterize the 3D printed valves which showed that they capable of precise liquid flow control and on/off operation. We envision that this technique can be applied to fabricating more complex fluidic components such as micropumps and multiplexers, thus further advancing the capabilities of 3D printed microfluidics.

ACKNOWLEDGMENTS

This work was partially supported by the Bill and Melinda Gates Foundation. We thank Brian Wright for his technical assistance with multi-material 3D printing.

REFERENCES

[1] S. K. Sia and G. M. Whitesides, "Microfluidic devices fabricated in Poly(dimethylsiloxane) for biological studies," *Electrophoresis*, vol. 24, no. 21, pp. 3563-3576, Nov. 2003.

[2] H. Andersson and A. V. D. Berg, "Microfluidic devices for cellomics: a review," *Sensors and Actuators B*: Chemical, vol. 92, no. 3, pp. 315-325, Jul. 2003.

[3] C. Yi, C. W. Li, S. Ji and M. Yang, "Microfluidics technology for manipulation and analysis of biological cells," *Analytica Chimica Acta*, vol. 560, no. 1-2, pp. 1-23, Feb. 2003.

[4] D. Erickson and D. Li, "Integrated microfluidic devices," *Analytica Chimica Acta*, vol. 507, no. 1, pp. 11-26, Apr. 2004.

[5] A. W. Martinez, S. T. Phillips, G. M. Whitesides and E. Carrilho, "Diagnostics for the developing world: microfluidic paper-based analytical devices," *Anal. Chem.,* vol. 82, no. 1, pp. 3-10, Jan. 2010.

[6] P. S. Dittrich and A. Manz, "Lab-on-a-chip: microfluidics in drug discovery," *Nature Reviews Drug Discovery*, vol. 5, no. 3, pp. 210-218, Mar. 2006.

[7] B. H. Weigl, R. L. Bardell and C. R. Cabrera, "Lab-on-a-chip for drug development," *Advanced Drug Delivery Revires*, vol. 55, pp. 349-377, 2003.

[8] G. M. Whitesides, "The origins and the future of microfluidics," *Nature*, vol. 442, no. 7101, pp. 368-373, Jul. 2006.

[9] Y. Xia and G. M. Whitesides, "Soft Lithography," *Annu. Rev. Mater. Sci*., vol. 28, pp. 153-184, 1998.

[10] D. Qin, Y. Xia and G. M. Whitesides, "Soft lithography for micro-and nanoscale patterning," *Nature Protocols*, vol. 5, no. 3, pp. 491-502, Feb. 2010.

[11] R. S. Kane, S. Takayama, E. Ostuni, D. E. Ingber and G. M. Whitesides, "Patterning proteins and cells using soft lithography," *Biomaterials*, vol. 20, no. 23-24, pp. 2363-2376, Dec. 1999.

[12] M. A. Unger, H. Chou, T. Thorsen, A. Scherer and S. R. Quake, "Monolithic microfabricated valves and pumps by multilayer soft lithography," *Science*, vol. 288, no. 5463, pp.113-116, Apr. 2000.

[13] A. K. Au, W. Huynh. L. F. Horowitz and A. Folch, "3D-printed microfluidics," *Angew Chem Int Ed Engl.*, vol. 55, no.12, pp. 3862-3881, 2016.

[14] J. L. Erkal et al, "3D printed microgluidic devices with integrated versatile and reusable electrodes," *Lab Chip*, vol. 14, no. 12, pp. 2023 – 2032, 2014.

[15] P. J. Kitson, M. H. Rosnes, V. Sans, V. Dragone and L. Cronin, "Configurable 3D-printed milifluidic and microfluidic 'lab on a chip' reactionware devices," *Lab Chip*, vol. 12, no. 18, pp. 3267-3271, 2012.

[16] T. Y. Lin, T. Do, P. Kwon and P. B. Lillehoj, "3D printed metal molds for hot embossing plastic microfluidic devices," *Lab Chip*, vol. 17, no. 2, pp. 241-247, 2017.

[17] M. D. Symes et al, "Integrated 3D-printed reactionware for chemical synthesis and analysis," *Nature Chemistry*, vol. 4, no. 5, pp. 349-354, Apr. 2012.

[18] C. I. Rogers, K. Qaderi, A. T. Wolley and G. P. Nordin, "3D printed microfluidic devices with integrated valves," *Biomicrofluidics*, vol. 9, no. 1, p. 016501, Jan. 2015.

[19] A. Au, N. Bhattacharjee, L. F. Horowitz, T. C. Chang and A. Folch, "3D-printed microfluidic automation,"*Lab Chip*, vol. 15, no. 8, pp. 1934-1941, 2015.

[20] H. Gond, A. T. Woolley and G. P. Nordin, "High density 3D printed microfluidic valves, pumps, and multiplexers," *Lab Chip*, vol. 16, no. 13, pp. 2450-2458, 2016.